

Embracing defects and disorder in magnetic nanoparticles

*Aidin Lak,^{*a} Sabrina Disch^{*b} and Philipp Bender^{*c}*

^aDepartment of Physics and Center for NanoScience, LMU Munich, Amalienstr. 54, 80799 Munich, Germany.

^bDepartment für Chemie, Universität zu Köln, Luxemburger Strasse 116, 50939 Köln, Germany.

^cDepartment of Physics and Materials Science, University of Luxembourg, 162A avenue de la Faïencerie, L-1511 Luxembourg, Grand Duchy of Luxembourg.

E-mails: lak.aidin@lmu.de, sabrina.disch@uni-koeln.de, philipp.bender@uni.lu

All three authors contributed equally to the manuscript.

Abstract

Iron oxide nanoparticles have tremendous scientific and technological potential in a broad range of technologies, from energy applications to biomedicine. To improve their performance, single-crystalline and defect-free nanoparticles have thus far been aspired. However, in several recent studies defect-rich nanoparticles outperform their defect-free counterparts in magnetic hyperthermia and magnetic particle imaging. Here, an overview on the state-of-the-art of design and characterization of defects and resulting spin disorder in magnetic nanoparticles is presented with a focus on iron oxide nanoparticles. The beneficial impact of defects and disorder on intracellular magnetic hyperthermia performance of magnetic nanoparticles for drug delivery and cancer therapy is emphasized. Defect-engineering in iron oxide nanoparticles emerges to become an alternative approach to tailor their magnetic properties for biomedicine, as it is already common practice in established systems such as semiconductors and emerging fields including perovskite solar cells. Finally, perspectives and thoughts are given on how to deliberately induce defects in iron oxide nanoparticles and their potential implications for magnetic tracers to monitor cell therapy and immunotherapy by magnetic particle imaging.

Keywords: iron oxide nanoparticles, magnetic hyperthermia, defect-engineering, design-by-disorder, magnetic spin disorder

1. Introduction

Despite their common negative connotation, *defects* and *disorder* can be highly desirable in nature and materials design^[1]. Colorful examples for nature's *design-by-disorder* are butterfly wings, whose vibrant colors originate from slightly disordered arrangements of photonic crystals^[2], and white beetle scales, whose exceptional whiteness is caused by a very high degree of disorder^[3]. Having learned from nature, mimicking its powerful *design-by-disorder* strategy has become an emerging field of research in materials science^[4]. This design method has led to novel applications e.g. within the field of disordered photonics^[5]. Nowadays, defect-engineering is commonly used in designing semiconductors^[6], perovskite solar cells^[7], metals^[8], multiferroics^[9], nanocomposites^[10], and carbon materials^[11,12] to tailor functional properties. Recent years have witnessed ground-breaking work in this area^[13–16], focusing exclusively on exploiting structural disorder in various functional materials such as metal-organic frameworks to optimize specific material characteristics. Notably, the electronic structure of condensed matter is significantly affected by intrinsic defects such as vacancies, impurities, and dislocations^[17], which in turn modify macroscopic material characteristics, including optical^[18] and magnetic properties e.g. by domain wall pinning^[19].

However, for magnetic materials changing our negative perception about defects has had a much slower pace than other fields. Recently, the generic relevance of the *defect-induced* Dzyaloshinskii–Moriya interaction (DMI) for the spin microstructure of defect-rich ferromagnets was verified^[20], suggesting a potential for creation of local chiral spin textures, i.e. skyrmions^[21], in all kinds of disordered magnetic materials. Magnetic materials offer wide-spread novel

technological potential^[22], with magnetic nanoparticles^[23], especially iron oxide nanoparticles, being indispensable candidates for varieties of biomedical applications^[24], including magnetic hyperthermia^[25], and magnetic particle and resonance imaging (MPI^[26], MRI^[27]).

To assess and optimize the performance of magnetic nanoparticles, it is crucial to consider their structure and magnetism on a variety of length scales, ranging from the atomistic to the macroscopic regime (**Figure 1**). While considering magnetic nanoparticles as mesoscale dipoles is sufficient to understand the qualitative principle of magnetic hyperthermia and MPI, the internal MNP structure directly impacts magnetic properties and, hence, magnetic hyperthermia and MPI performance. Due to their large surface to volume ratio, magnetic nanoparticles are particularly prone to structural and compositional defects,^[28] and thus synthesis of defect-free magnetic nanoparticles remains highly challenging.^[29] From very early aqueous synthesis of iron oxide nanoparticle suspensions through a co-precipitation method,^[30] there have been enormous efforts on controlling physicochemical properties, often with the goal to prepare single-crystalline iron oxide nanoparticles.^[31] To date, the synthesis of defect-free iron oxide nanoparticles remains the golden standard in colloidal chemistry.

Recently, however, it was demonstrated that in case of magnetic hyperthermia (and also MPI, MRI) defect-rich iron oxide nanoparticles can actually outperform their defect-free counterparts.^[32–39] Motivated by these striking results, here, we will remove the common stigma of defects in iron oxide nanoparticles. At first, we discuss recent studies on positive impacts of defects and disorder on magnetic hyperthermia performance of iron oxide nanoparticles. Next, we review the magnetic spin disorder in iron oxide nanoparticles associated with defects and disorder. Finally, we present an overview about the state-of-the-art on how to incorporate and induce defects in iron oxide nanoparticles.

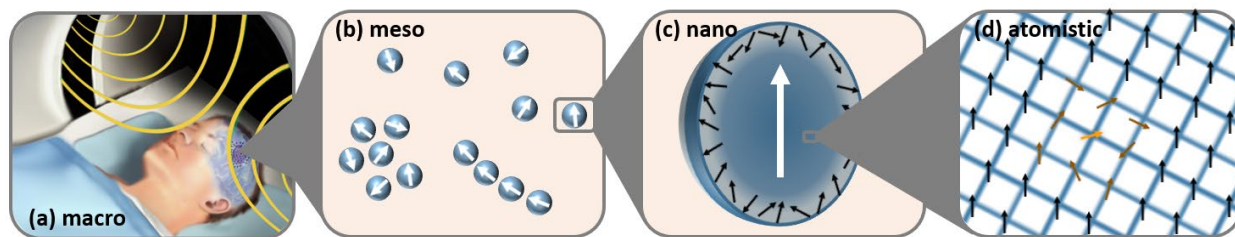


Figure 1. Multiple length scales in magnetic nanoparticles. (a) The macroscopic application (here: magnetic hyperthermia for the treatment of glioblastoma) can be understood qualitatively by considering magnetic nanoparticles on the mesoscale as magnetic dipoles (b) of the respective bulk material with nanosized dimensions. Quantitatively, magnetic nanoparticles performance is critically affected by spin disorder on both (c) the nanoscale (i.e. its distribution within the particle from surface into the particle interior) and (d) the atomistic scale (e.g. site-defect induced spin disorder). As shown e.g. in^[63], defects in the crystalline structure cause atomistic spin disorder, that can critically modify the magnetic properties of nanoparticles and hence influence the macroscopic ensemble properties and therefore their magnetic hyperthermia performance. Panel (a) reproduced from^[45].

2. Iron oxide nanoparticles in biomedicine

2.1. Designing the ideal iron oxide nanoparticles for magnetic hyperthermia

Iron oxide nanoparticles transduce magnetic energy to heat through magnetic losses when exposed to external alternating magnetic fields. They can therefore serve as remotely activated, nanometric heat sources^[40] to eradicate cancer cells after being intracellularly engulfed.^[25,41] Remarkably, the concept of exploiting iron oxide nanoparticles as local heat sources has been recently expanded to other technologies such as catalysis,^[42] water electrolysis,^[43] and local polymerization.^[44]

Magnetic hyperthermia is especially attractive for the treatment of inoperable tumors such as glioblastoma (illustrated in Figure 1a), the most common and a highly aggressive brain cancer.^[45]

Although magnetic hyperthermia is not yet a routine treatment, clinical trials are ongoing. With the clinical application of magnetic hyperthermia in mind, the following restrictions need to be considered regarding particle design to optimize the heating:^[46] (1) focus on biocompatibility^[47] and biodegradation: iron oxide nanoparticles are hitherto the only clinically approved heat transducers to be administered to humans.^[48] (2) focus on Néel relaxation: iron oxide nanoparticles have to preserve their heating performance when intracellularly immobilized, as in the cellular

milieu a physical rotation of nanoparticles, i.e. Brownian relaxation, is mostly inhibited.^[49-51] (3) focus on high-frequency and low-amplitude alternating fields: intracellularly immobilized iron oxide nanoparticles should induce hyperthermic effects, i.e. rising temperature to $\sim 42^\circ\text{C}$, but also comply with the biological safety limits.^[52] Currently, most magnetic hyperthermia devices approved for clinical trials apply magnetic fields within a frequency range of 0.05-1.2 MHz and an amplitude range of 0-5 kA/m.^[53]

The macroscopic heating power of an iron oxide nanoparticle ensemble is usually given by the specific absorption rate $SAR = f \cdot S/c$, where $S = \mu_0 \oint M(H)dH$ is the area of alternating field hysteresis loops, and c is the weight concentration of the magnetic material.^[54] To better compare results from different experimental setups, the intrinsic loss parameter ILP was introduced, which is given by $ILP = SAR/(\mu_0 H_0^2 f)$.^[55,56] Within the framework of the linear response theory, that is at first approximation valid in case of low amplitudes, the ILP is given by $ILP = \pi\mu_0\chi''(\omega)/c$, where $\chi''(\omega)$ is the imaginary part of the complex susceptibility.^[57] It has been shown that in case of single-crystalline maghemite, when dispersed in highly viscous media, 14-nm nanoparticles exhibit the maximum heating performance at the frequency and field amplitude of 1000 kHz and 24.8 kA/m.^[58] Note that mesoscale ensemble effects such as arrangement,^[59] interactions,^[60] and alignment^[61,62] can lead to deviations. Recently, Lappas et al.^[63] observed that the magnetic heating of 10-nm iron oxide nanoparticles is increased by structural point defects inside the crystal lattice (sketch in Figure 1d). In this case the improved heating compared to defect-free particles is explained by increased effective magnetic anisotropy KV thanks to individual point defects.

To further increase magnetic heating, iron oxide nanoparticles with large moments are desired. Large, thermally blocked iron oxide nanoparticles could have a higher heating power than superparamagnetic iron oxide nanoparticles, however only at driving field amplitudes larger than

their coercive fields,^[64] i.e. much larger than 5 kA/m. For this reason, we propose the use of large and magnetically *soft* iron oxide nanoparticles, so that they have an appreciable response $\chi''(\omega)$ at low field amplitudes.

A possible approach to reduce the effective anisotropy KV , and hence increase the initial susceptibility, is the introduction of structural defects. This can be achieved for example by 2D defects in the crystal structure, such as grain boundaries and stacking faults. This approach is well established for iron-based bulk ferromagnets, for which magnetic softening (i.e. decrease of coercivity) can be achieved by decreasing the grain size below the material specific magnetic correlation length.^[65–68] Further potential strategies include doping and interfaces, as discussed below.

2.2. Defect-rich iron oxide nanoparticles which excel at magnetic hyperthermia

Structural defects, which are routinely found in iron oxide nanoparticles, include vacancies, twinning defects,^[69] grain boundaries, and interfaces.^[31,63,69–73] Iron oxide nanoparticles synthesized by thermal decomposition method tend to have defected structure and interfaces that can lead to anomalous magnetic properties.^[74,75] **Figure 2** shows exemplarily 23 nm iron oxide nanocubes synthesized by thermal decomposition of iron oleate^[37,74] Combining high angle annular dark field scanning transmission electron microscopy (HAADF-STEM), X-ray diffraction (XRD), and electron energy loss spectroscopy (EELS), it has been observed that thermal annealing of PEGylated nanocubes at 80°C for 48 h induces Fe²⁺ vacancies in the particle crystal structure. The Fe²⁺ vacancies together with ever remaining FeO-subdomains within the particles led to comparatively small effective magnetic anisotropy KV . Remarkably, the thermally treated nanocubes preserved their improved intracellular magnetic hyperthermia, as evaluated by *in-vitro* SAR measurements during interaction and uptake by IGROV-1 breast cancer cells (Figure 2k).

Note that single-phase magnetite nanocubes with same size lose their heating performance nearly completely in viscous media.^[76] Thus, these mildly treated nanocubes can be regarded as the prototype for improved magnetic heating by *defect-induced* magnetic softening.

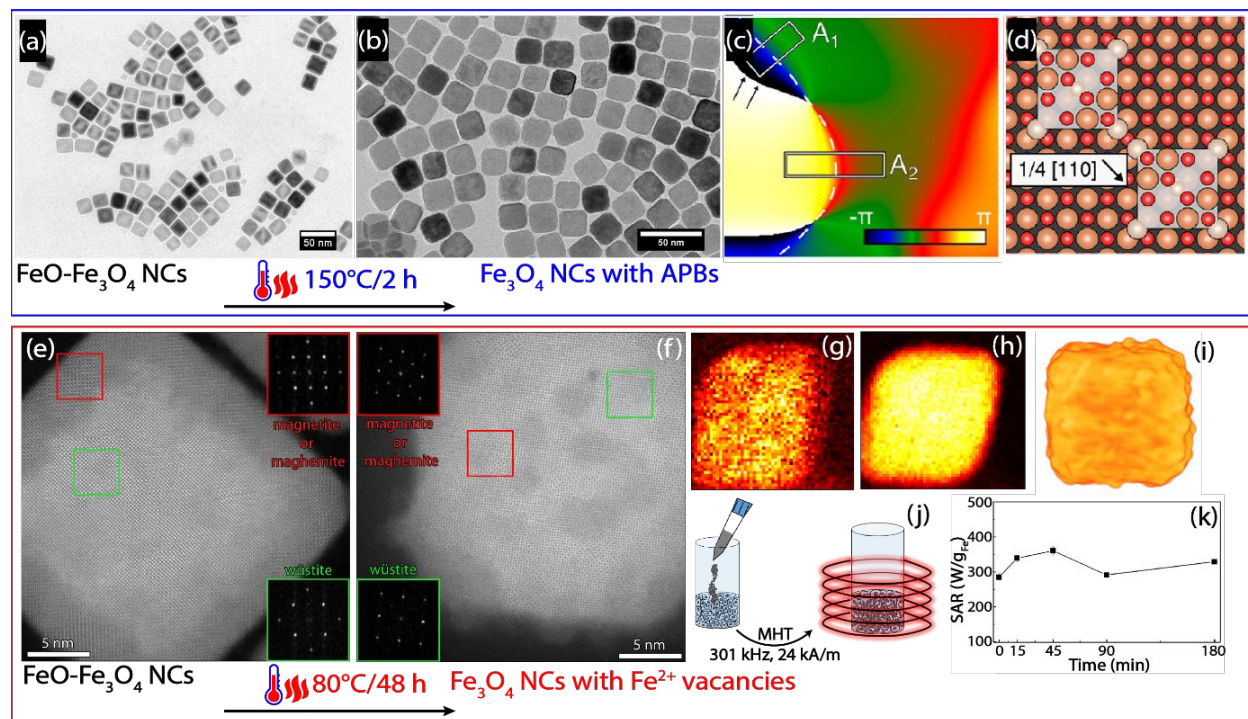


Figure 2. Thermally induced antiphase boundary (APB) defects and cation vacancies in iron oxide nanocubes synthesized via thermal decomposition of iron-oleate. Low resolution TEM images of (a) as-prepared FeO-Fe₃O₄ core-shell nanocubes and (b) thermally annealed nanocubes at 150°C for 2 h. (c) Phase map of {220} spinel-exclusive fringe of a Fourier filtered HRTEM image of a single particle acquired by geometric phase analysis (GPA), indicating an APB with the dashed line, that is formed where two growing magnetite sub-domains coalescent. (d) Scheme of unit cells of two Fe₃O₄ domains (white rectangles) nucleated on an ideal FeO surface that are shifted by 1/4 [110]. Adapted with permission from^[74]. Copyright 2013, American Chemical Society. (e) High-resolution HAADF-STEM image of an FeO-Fe₃O₄ core-shell nanocube: insets are Fourier analysis diffraction patterns of regions containing FeO and magnetite/maghemite. (f) High-resolution HAADF-STEM image of a nanocube after 48 h annealing at 80°C: insets are Fourier analysis diffraction patterns of regions containing FeO and magnetite/maghemite. (g) Fe²⁺ and (h) Fe³⁺ valency maps of a single thermally treated nanocube obtained by fitting the electron energy loss spectra of each pixel to the reference spectra. (i) Three-dimensional visualization of the individual nanocube shown in (f), which was reconstructed using electron tomography technique. (j) Scheme of evaluating *in-vitro* magnetic hyperthermia performance of thermally treated nanoparticles during interaction and uptake by IGROV-1 breast cancer cells. (k) Evolution

of SAR values as a function of the incubation time were measured at field frequency and amplitude of 301 kHz and 24 kA/m. The SAR is virtually independent of nanoparticle cell internalization and immobilization. Adapted with permission from^[37]. Copyright 2018, American Chemical Society.

Flower-shaped iron oxide nanoparticles^[32,33] represent a different, prominent example for large, defect-rich iron oxide nanoparticles. As can be seen in **Figure 3a,b,c**, the nanoflowers are 20-100 nm aggregates consisting of small ~ 5-15 nm maghemite crystallites.^[77] The small crystallites are separated by grain boundaries, as highlighted by the dashed lines in Figure 3b. For this reason, the nanoflowers are often classified as multicore particles.^[48,78] However, because of their dense structure, they can be also regarded as individual magnetic nanoparticles but with a nanocrystalline substructure. Due to exchange interactions between the small crystallites (Figure 3b, dashed lines), the atomic moments within the total particle volume are preferentially magnetized along the same direction, leading to large effective moments at low fields. As a result of the grain boundaries, however, the nanoflowers exhibit a significant internal spin disorder,^[35] something which is also observed for nanocrystalline bulk samples of Ni.^[79] This spin disorder results in nearly vanishing coercivities,^[80] analogous to nanocrystalline bulk ferromagnets.^[65-68] Consequently such nanoflowers, and similar dense iron oxide nanoparticle aggregates, excel at magnetic hyperthermia at low field amplitudes.^[32-36,80-82] We attribute the increased heating to the magnetic softening, which results in increased $\chi''(\omega)$ at low field amplitudes similar to single-core thermally treated nanocubes discussed before (Figure 2).

An additional remarkable feature of nanoflowers is that their already outstanding heating performance can even be further increased with magnetic interactions at the mesoscale.^[34] This can be related to a parallel alignment between neighboring particle moments within dense aggregates^[83]. This behavior is in contrast to conventional interacting iron oxide nanoparticle systems (i.e. dense powder samples of single-core particles), in which an antiparallel alignment of

neighboring particle moments has been observed^[84,85], culminating in reduced susceptibility and decreased heating^[86].

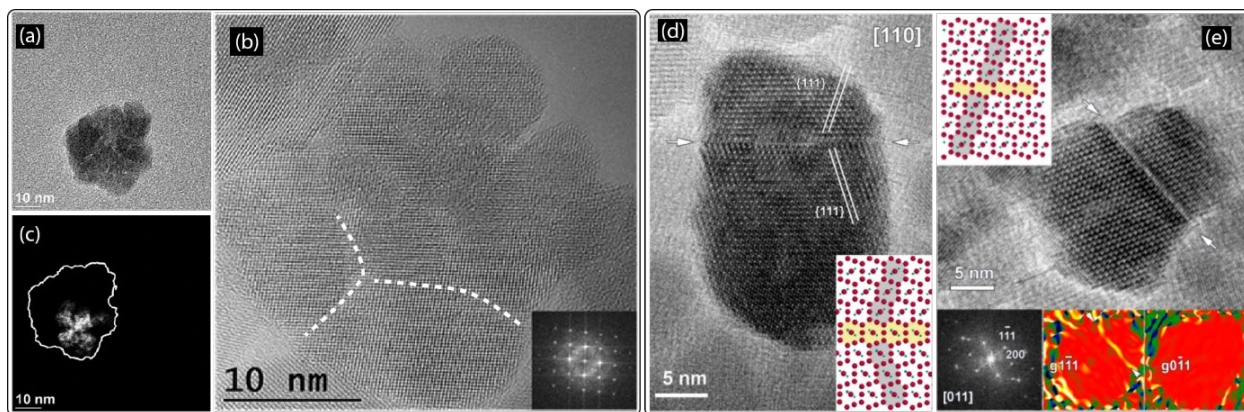


Figure 3. Grain boundaries and twinning defects in iron oxide nanoparticles. (a) Typical TEM micrograph of an individual nanoflower-shaped iron oxide nanoparticle synthesized via polyol process. (b) HRTEM micrograph of a single flower-like nanoparticle, so-called nanoflower. The dashed lines indicate grain boundaries between domains (c) Dark-field TEM micrograph of an individual particle showing that domains sharing the same crystallographic orientation varies between 5 to 15 nm in size. While each domain is well coherent, domains are oriented differently with respect to each other. (d) HRTEM micrograph of an iron oxide nanoparticle synthesized via hydrothermal method. The nanoparticle shows a twinning defect along (111) plane, as indicated by white arrows. Inset shows atoms arrangement along the twinning plane that is highlighted in yellow. The flipping of the atomic arrangement of Fe_3O_4 around the (111) twinning plane is apparent. (e) HRTEM micrograph of a so-called dimer iron oxide nanoparticle synthesized via hydrothermal method, showing a grain boundary defect along (111) crystalline plane. Inset at the top shows atoms arrangement along the grain boundary, that is colored in yellow. Inset at the bottom-left presents Fourier-transform diffraction pattern and insets at the bottom-right show GPA maps of $g_{1\bar{1}1}$ and $g_{0\bar{1}1}$ planes. The left side GPA map indicates lattice distortion along the grain boundary plane i.e. (111), as seen by a discontinuity in the color map at the grain boundary. No lattice distortion is observed along out-of-grain boundary planes e.g. (011), as shown in the right side GPA color map. Panels (a,c) adapted with permission from^[35]. Copyright 2018, American Chemical Society. Panel (b) adapted with permission from^[33]. Copyright 2012, American Chemical Society. Panels (d,e) adapted with permission from^[69]. Copyright 2014, American Chemical Society.

As highlighted above, there are multiple iron oxide nanoparticle systems in which structural defects contribute positively to enhancing the performance for biomedical applications that are

based on the Néel relaxation mechanism such as magnetic hyperthermia and MPI. In the following, we will review the interrelation of structural and spin disorder in magnetic nanoparticles that is expected to be decisive for their functionality. We will then expand our discussion on the current status regarding defect-engineering in iron oxide nanoparticles, to postulate new pathways for exploiting structural defects in favor of particle performance in biomedical applications.

3. Defect-induced spin disorder in iron oxide nanoparticles

In the previous section we introduced several examples of structurally disordered iron oxide nanoparticles that exhibit greatly enhanced performance in biomedical applications, in particular magnetic hyperthermia. Structural deviations from homogeneity can cause atomistic disorder of the magnetic spin ensemble and thus significantly alter the particle properties. In addition, nanoscale surface effects naturally play a decisive role in nanoparticles due to large surface-to-volume-ratio which can also cause localized spin disorder. The spin disorder in magnetic nanoparticles thus needs to be addressed to fully understand the interrelation between defects and disorder and the technological performance of magnetic nanoparticles. Despite recent advances in both microscopy and scattering approaches, resolving the magnetization configuration at the nanoscale^[87], including the complex spin configuration within magnetic nanoparticles, remains a key challenge in nanomagnetism.

Whereas long-range order is routinely characterized using diffraction techniques assuming periodic boundary conditions, the local, short range nature of disorder effects requires combination of a variety of techniques on different length scales as well as a model adapted to the length scale that is probed. Structural defects within individual magnetic nanoparticles are typically investigated with high-resolution electron microscopy techniques^[71] (**Figure 4a,b**) whereas X-ray

techniques such as XRD^[63] or X-ray circular dichroism (XMCD)^[88] can be used to obtain ensemble-averaged information regarding stoichiometry and crystal structure.

Methodology towards spin disorder includes magnetometry^[89], Mössbauer^[90] & Raman^[91] spectroscopy, nuclear magnetic resonance (NMR)^[92], Lorentz transmission electron microscopy (LTEM)^[93], high-resolution electron loss spectroscopy (HR-EELS)^[70], and magnetic neutron diffraction^[94] and small-angle neutron scattering (SANS)^[95]. Each of these techniques can provide unique information but only at specific length scales. Therefore, often combinations of various techniques are needed to acquire a self-consistent picture.

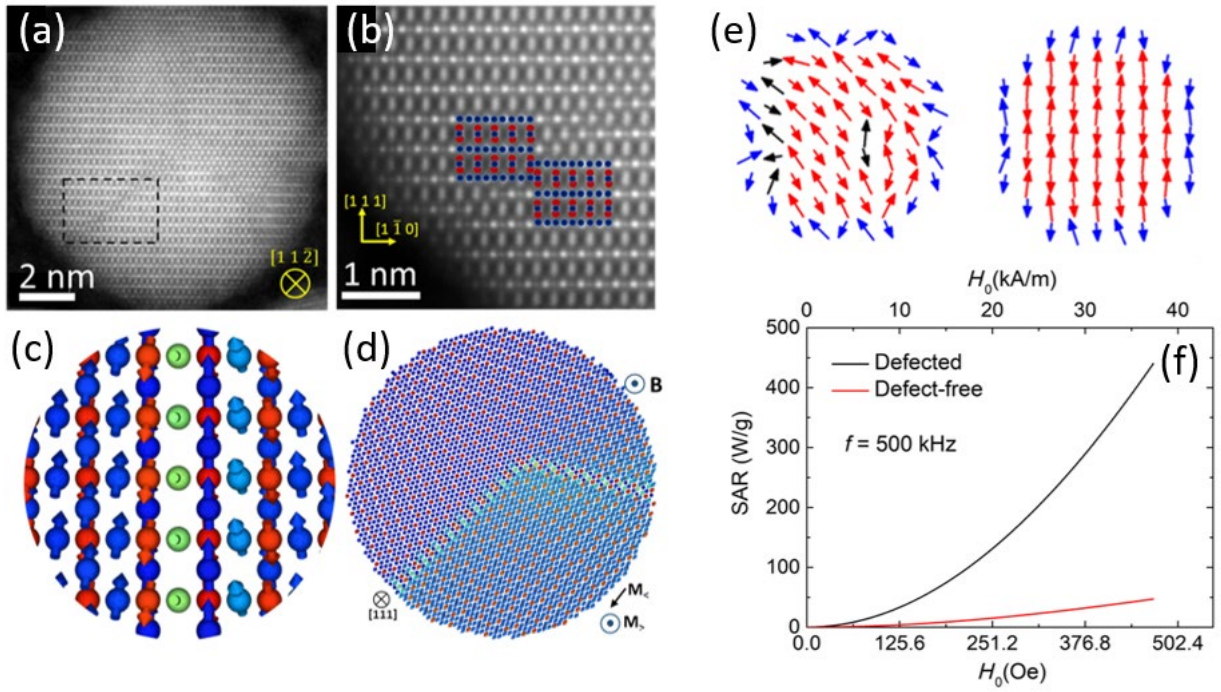


Figure 4. From structural defects in nanoparticles to spin disorder and enhanced magnetic heating performance. (a) Anti-phase boundary in a representative iron oxide nanoparticle, atomically resolved using HAADF STEM. (b) magnification of the dashed area indicated in (a). (c,d) Atomistic spin calculations of illustrate the spin misalignment near antiphase boundaries in model nanoparticles. (e) Monte Carlo simulation of the spin ensemble in a defected (left) and a defect-free nanocrystal (right) near field reversal after saturation. (f) Specific absorption rate calculated for a defected and a defect-free nanoparticle. Panels (a-d) and (e,f) reproduced from^[71] and^[63], respectively.

3.1. Spin disorder at different scales

The existence of spin disorder in nanoparticles is typically concluded from low magnetization as compared to the bulk materials^[89,96], accompanied by non-saturating magnetic behaviour^[97] and exchange biasing^[98], all observed using macroscopic magnetization measurements. Microscopic information on spin disorder, i.e. atomic spins deviating from the collinear order of the material, is accessible through the hyperfine structure of in-field Mössbauer spectroscopy^[99]. In combination with macroscopic magnetization and X-ray diffraction, the generally assumed nanoscale model of a collinear macrospin surrounded by surface-near spin disorder (Figure 1c) is

typically applied^[100–103]. Surface spin disorder is understood as a result of broken exchange bonds and low symmetry near the particle surface. Moreover, the correlation of structural and spin disorder is widely accepted. Within the macrospin model, spin disorder is hence mostly attributed to surface effects based on a particle size dependence of macroscopic magnetization properties, or based on a structurally coherent magnetic grain size smaller than the particle itself, as accessible through neutron diffraction^[94]. To unambiguously confirm the location of spin disorder near the particle surface, spatially sensitive techniques are required with nanometer resolution.

LTEM provides information on the stray field magnetization with spatial resolution of a few nm and can hence be applied to individual particles with sizes as small as a few nm^[93]. Electron holography provides higher spatial resolution and is sensitive to the entire nanoparticle spin configuration and has been applied to the magnetic interparticle coupling in arrangements of nanoparticles^[104]. On the individual nanoparticle level, high-resolution magnetic maps of individual Fe nanocubes have been generated to reveal the size-induced transition between vortex (**Figure 5a-c**) and single-domain states (Figure 5d-f) within the nanoparticles^[105]. Whereas defect-free nanoparticles have been targeted for such proof-of-principle studies, application of electron holography techniques to the defect-induced spin structure in magnetic nanoparticles will be a challenging and highly interesting endeavor. HR-EELS is both spatially and element-sensitive and has elucidated the site-dependent surface spin canting in cobalt ferrite nanoparticles, revealing surface spin canting for the cobalt sites, but not for the iron sites^[70].

Magnetic SANS is sensitive to nanoscale magnetic fluctuations with sub-Å spatial resolution, giving access to the spatially resolved magnetization distribution as well as directionally resolved magnetization correlations in magnetic nanoparticles^[95]. Through the spatial sensitivity with length scales of 0.1 – 500 nm, surface spin disorder^[106] and correlated surface spin canting^[107,108]

become accessible. Using magnetic SANS, a significant reduction of surface spin disorder was found upon cooling to low temperatures of 10 K^[109]. More recently, a strong field-dependence of surface spin disorder was revealed, expressed by a gradual polarization of initially disordered surface spins even beyond the structurally coherent grain size (Figure 5h)^[110]. The field dependence of the spatial distribution of surface spin disorder ultimately gives access to the spatially resolved disorder energy towards the particle surface^[110].

Nanoscale surface effects have recently been exploited towards hollow nanoparticles. The high magnetic disorder in these particle shells was attributed to two antiferromagnetically coupled noncollinear structures close to speromagnets based on a broad distribution of hyperfine fields as determined from Mössbauer spectroscopy^[111].

3.2. Spin disorder – correlated or not?

Depending on surface and magnetocrystalline anisotropies, different types of spin canting towards the particle surface have been suggested by theory, including so-called artichoke, throttled, and hedgehog spin structures^[112]. However, experimental evidence for such structures is scarce. The size-dependent spin structures in manganese-zinc ferrite nanoparticles were studied using unpolarized SANS in combination with micromagnetic simulations, revealing increased magnetic inhomogeneity with particle size and correlated, non-collinear spin states occurring for particle sizes beyond 20 nm^[113].

Correlated spin canting has been reported for assemblies of smaller, ~10 nm nanoparticles^[107,108], without directly discriminating one of the suggested spin structures. In contrast, non-interacting ferrite nanoparticles of similar size reveal random surface spin disorder without a traceable coherent transversal magnetization component^[110]. In consequence, a strong impact of interparticle

interactions on spin disorder and spin canting is evident and needs to be considered for applications of spin disorder towards magnetic heating.

3.3. Spin disorder in the particle interior

Whereas the commonly accepted macrospin model including surface spin disorder is sufficient to explain a large fraction of macroscopic phenomena, the potential existence of atomistic spin disorder in the particle interior (Figure 1d) is often disregarded. The spin disorder distribution within magnetic nanoparticles is only accessible using techniques that are both quantitative and spatially sensitive. Indeed, polarized SANS has revealed significant contributions of spin disorder even in the particle interior^[114], expressed as a reduced local magnetization in the particle core^[106,109,110]. In several reports, the spin disorder in the particle interior has even been found to dominate surface spin disorder^[106,115]. Such a reduced magnetization has been attributed to canting of Fe moments in both tetrahedral and octahedral sites, revealed by a combination of NMR and Mössbauer spectroscopies, and related to reversed moments and frustrated topology^[92].

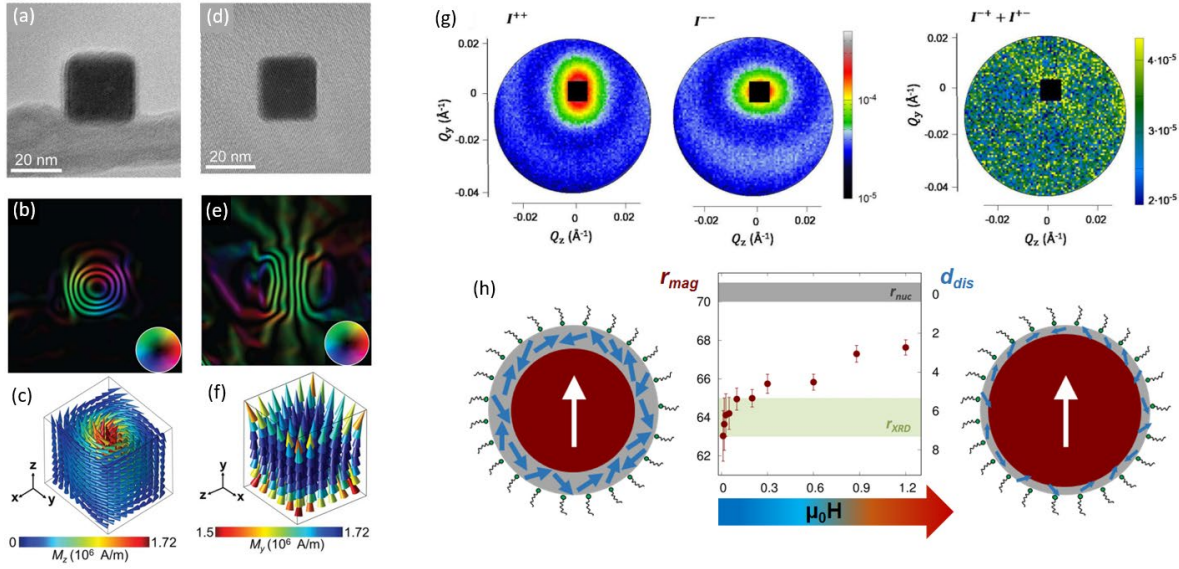


Figure 5. Nanoscale magnetization in magnetic nanoparticles. (a-f) Magnetic electron holography of vortex (a-c) and single-domain (d-f) spin configurations in Fe nanoparticles. (a,d) Experimental hologram, (b,e) magnetic induction flux line maps derived from the experimental phase image (inset: color wheel indicating the direction of the magnetic induction). (c,f) Micromagnetic simulation of the 3D magnetization of a 29.5^3 nm^3 and a $24 \times 26 \times 24 \text{ nm}^3$ Fe nanocube in equilibrium state, indicating the vortex and single-domain configurations, respectively. Adapted with permission from^[105]. Copyright 2015, American Chemical Society. (g) Magnetic SANS data by cobalt ferrite nanoparticles in applied magnetic field of 1.2 T. The non-spin-flip channels I^{++} and I^{--} give access to the structural morphology and collinear magnetization distribution (*i.e.* the magnetization component parallel to the applied field). The spin-flip channels I^{+-} and I^{-+} provide a combination of collinear magnetization and spin misalignment. (h) Field dependence of the thickness d_{dis} of the surface-near spin disorder shell in ferrite nanoparticles. In increasing applied magnetic field, the size of the collinearly magnetized nanoparticle core r_{mag} overcomes the structurally coherent grain size r_{XRD} , leaving a reduced shell of spin disorder. Panels (g,h) adapted with permission from^[110].

A clear particle size dependence of spin disorder in iron oxide nanoparticles has been established using Mössbauer spectroscopy, revealing enhanced spin canting in an intermediate particle size of 8-12 nm^[31]. Combination of magnetic SANS with nuclear resonance X-ray scattering has further revealed a clear atomic site dependence of the spin misalignment^[115]. The significant amount of spin disorder found in the nanoparticle interior underlines that disorder and defects on the atomic

scale are highly relevant to understand and control the nanoscale and macroscopic magnetic properties in nanoparticles.

Indeed, structural distortions changing the local coordination geometry in the vicinity of defects have a direct influence on interatomic exchange and hence spin disorder^[116]. For ferrite nanoparticles, strong variations of the degree of spinel inversion are commonly observed^[117–121]. The synthesis technique has been reported to substantially influence the ferrite nanoparticle magnetization and, hence, also the spin disorder^[71], through structural defects such as antiphase boundaries resulting from topotactic oxidation from FeO to maghemite^[74] (see Figure 2a-d and 4a-d). Antiphase boundaries have further been found to induce local ferromagnetic coupling and enhance the magnetic properties of magnetic nanoparticles^[122]. Local disorder in core-shell $\text{Fe}_x\text{O}_{3-\delta}\text{O}_4$ nanocrystals has recently been discovered by analysis of the atomic pair distribution function and correlated with atomistic spin disorder and enhanced magnetic heating efficiencies^[63] (Figure 4e,f). All these findings illustrate that for a comprehensive understanding of the macroscopic performance of magnetic nanoparticles, it is indispensable to consider both structural and spin disorder on a variety of length scales (Figure 1), including the nanoscale magnetization distribution, but also the atomistic scale defect-induced disorder in magnetic nanoparticles.

Having established the potential of structural and magnetic disorder for improved magnetic hyperthermia performance, we next highlight current synthetic approaches on how to deliberately engineer defects and disorder in iron oxide nanoparticles.

4. Defect-engineering in iron oxide nanoparticles

4.1. Colloidal synthesis: a journey toward disordered iron oxide nanoparticles

The quest to synthesize defect-free and single-crystalline magnetic nanoparticles dates back to almost twenty years ago when the first colloidal thermal decomposition syntheses emerged.

Varieties of organometallic precursors including $\text{Fe}(\text{C}_6\text{H}_5\text{N}(\text{O})\text{NO})_3$ ^[123], $\text{Fe}(\text{CO})_5$ ^[124], $\text{Fe}(\text{acac})_3$ ^[125], $\text{FeO}(\text{OH})$ ^[126] and iron salts such as Fe(II) acetate^[127], have been used for synthesis of iron oxide nanoparticles. Large-scale size and shape-control synthesis of iron oxide nanoparticles have been realized after developing $\text{Fe}(\text{oleate})_3$ by Hyeon et al^[128]. Despite differing in solvent, capping ligands, and growth temperature, in these non-hydrolytic syntheses, nanoparticles are mostly a product of kinetically driven processes e.g. through adsorption/desorption of capping ligands on certain crystalline facets.^[129] Thanks to the kinetic pathways, the formation of uniformly sized and shaped iron oxide nanoparticles often takes no longer than an hour in these methods^[130]. However, detailed characterization studies have later revealed that $\text{Fe}(\text{CO})_5$, $\text{Fe}(\text{oleate})_3$, and Fe(II) acetate lead to $\text{FeO-Fe}_3\text{O}_4/\text{Fe}_2\text{O}_3$ and $\text{Fe-Fe}_3\text{O}_4$ ^[131] core-shell iron oxide nanoparticles with degraded magnetization and structural disorders^[127,132-135]. Several groups have developed twists in the decomposition chemistry^[136] and modified the synthesis involving protective gas^[137,138] to eliminate the paramagnetic FeO phase and obtain single-phase Fe_3O_4 nanoparticles. Further approaches reduce surface spin disorder in superparamagnetic ferrite magnetic nanoparticles by changing the nature of alkaline capping agents^[139].

Despite the progress, we know from solid state chemistry and materials science that defect-free crystals are the product of thermodynamically-driven processes, forming at much higher temperatures and longer reaction times than that of colloidal syntheses (i.e. 220-340°C, < 1h). Moreover, recent magnetic hyperthermia studies have strikingly shown that defect-free and highly crystalline single-core iron oxide nanoparticles lose nearly entirely their hyperthermia efficacy in highly viscous media^[76], *in-vitro*^[49], and intracellularly^[37,51]. Di Corato et al. have systematically

shown this phenomenon *in-vitro* for multicore and cubic-shape single-core iron oxide nanoparticles^[49].

The tendency to compare physicochemical properties of synthetic iron oxide nanoparticles such as saturation magnetization and magnetic anisotropy with the bulk-like properties has thus far distracted us from exploring defects and disorders in favor of biomedical applications. In the following, we will briefly discuss current synthetic approaches for defect- and disorder-engineering in single-phase and interfaces in core-shell iron oxide nanoparticles with particular focus on their impact on magnetic hyperthermia.

4.2. Defects and discontinuities induced by growth pathways

Capping ligands are an indispensable part of thermal decomposition syntheses, as they control size and morphology of nanocrystals by influencing the reaction kinetics. Playing with the binding nature and strength between capping agents and nanocrystals has always been an effective strategy to control particle shape and size^[140,141]. Recently, capping ligands were exploited to change the internal structure of iron oxide nanoparticles. A prime example is iron oxide nanoflowers (Figure 3a-c), wherein short length polyols such as diethylene glycol allows packing small crystallites into dense disordered structures, being separated by grain boundary defect (dashed lines in Figure 3b)^[77,142]. The effect of competition between short and long ligands on the particle structure has recently been shown in zinc ferrite nanoparticles. Increasing the ratio of acetylacetonone to oleic acid ligands results in assembly of small magnetic zinc ferrite subdomains into 100 nm cubic-particles, due to less bulkiness and higher mobility of acetylacetonone ligands as compared to oleic acid^[143]. Hydrothermally synthesized iron oxide nanoparticles showed to possess twinning and stacking faults defects (Figure 3d,e^[69]). Formation of twinning defects and stacking faults along (111) crystalline planes was attributed to the oriented-attachment crystal growth mechanism. A growth

mechanism similar to the nanoflowers was proposed for these defected iron oxide nanoparticles. The fusion of initial Fe_3O_4 crystallites, that is promoted by desorption of capping ligands, into a single particle accounts for twinning and stacking fault defects. Interestingly, none of these defects were observed when a similar synthesis mixture was treated by co-precipitation synthesis method. It was therefore discussed that an intensive activity and mobility of the capping ligands on crystallites, given to the synthesis reaction by high temperature hydrothermal reaction conditions, is required to form defect-rich iron oxide nanoparticles. Remarkably, it was demonstrated that iron oxide nanoparticles with stacking fault internal defects have a higher M_s and SAR than defect-free iron oxide nanoparticles^[69].

4.3. Defects and vacancies induced by oxidation

Most iron oxide nanoparticles synthesized via thermal decomposition syntheses have to some extent defects, disorders, and sub-domains. $\text{FeO-Fe}_3\text{O}_4$ core-shell nanoparticles, synthesized via the thermal decomposition of Fe(oleate)_3 and Fe(CO)_5 are the most heavily characterized iron oxide nanoparticle systems due to the synthesis robustness and particle size uniformity^[144]. Studies on post synthesis thermal treatment of these iron oxide nanoparticles toward single-phase iron oxide have led to new insights into oxidation-induced defects. It has been shown that the nucleation and growth of Fe_3O_4 on the FeO phase (i.e. the topotaxial oxidation from FeO to magnetite and maghemite) lead to formation of antiphase boundary (APB) defects at the interface between growing magnetite domains. Interestingly, APBs remained after four hours of thermal treatment at 150°C (Figure 2a-d)^[74]. The oxidation of core-shell iron oxide nanoparticles, synthesized by decomposition of Fe(CO)_5 , via mild cyclic magnetic stimulations has also resulted in the APBs^[145]. A step toward exploiting structural defects for biomedical applications was taken by mild thermal treatment of $\text{FeO-Fe}_3\text{O}_4$ nanoparticles after being capped with catechol-terminated functional

poly(ethylene glycol) polymers. A 48 hours thermal treatment at 80°C induced Fe²⁺ vacancies in the Fe₃O₄ phase of core-shell iron oxide nanoparticles, which result in the magnetic softening and thus the domination of the Néel relaxation. As discussed in the previous section, such a magnetic softening lead to improved magnetic hyperthermia performance of 23 nm cubic-shape particles compared to single-phase counterparts^[37] (Figure 2e-k).

4.4. Structural defects associated with interfaces and doping

Interfaces and doping are additional promising sources of breaking composition continuity and inducing atomic scale exchange interactions in magnetic nanoparticles. The magnetic anisotropy can be tuned by magnetic coupling in bi-magnetic hard-soft and soft-hard core-shell magnetic nanoparticles such as CoFe₂O₄-MnFe₂O₄^[146] and Fe₃O₄-CoFe₂O₄^[147]. Recently, trimagnetic Fe₃O₄-CoO-Fe₃O₄ core-shell-shell nanoparticles have been developed via seed-mediated thermal decomposition synthesis. Hard-soft exchange couplings at Fe₃O₄-Co doped ferrite and Co-doped ferrite-Fe₃O₄ interfaces largely influenced the superparamagnetic blocking temperature and magnetization hysteresis loops^[148].

An emerging approach to furthermore enhance magnetic exchange couplings is to tune the shell thickness. It was recently shown that forming an ultrathin shell of soft magnets (e.g. Fe₃O₄ and MnFe₂O₄) on CoFe₂O₄ nanoparticles leads to increased magnetic anisotropy^[149,150]. The shell thickness turned to be critical to observe a so-called enhanced spin canting phenomenon. Inserting a paramagnetic FeO interlayer spacer between Fe core and iron oxide shell in layered iron oxide nanoparticles was led to magnetostatic interactions between the core and the shell and enhanced magnetic hyperthermia performance^[73]. Despite being a promising approach, one has to bear in mind that synthesis of multi layered nanoparticles is much more challenging than those Iron oxide nanoparticles formed via one-pot reactions.

Breaking the cation ordering by substituting magnetic^[151] and non-magnetic ions into the iron oxide crystal structure has emerged as a strong tool to tune magnetic properties in the past years^[152,153]. For spinel ferrite nanoparticles, the cation distribution between A and B sites is decisive for the macroscopic magnetization, and strong variations of the inversion degree have been observed as nanoparticles often represent a non-equilibrium cation distribution^[117–119]. Zinc and manganese are the most commonly substituted cations into iron oxide nanoparticles^[154]. Despite being non-magnetic, Zn^{2+} replaces Fe^{3+} in tetrahedral crystalline sites and thus reduces antiferromagnetic couplings between Fe^{3+} in tetrahedral and octahedral sites. Depending on the ionic size and concentration of the substituting cation, lattice strain was induced in cobalt ferrite nanoparticles.^[155,156] Such approach appears promising to tailor the lattice strain and in result control the magnetization of iron oxide nanoparticles.

5. Conclusions and perspectives

The strong research interest on iron oxide nanoparticles is particularly driven by their unique potential for a wide range of biomedical applications. To optimize their magnetic properties, historically, the usual strategy has been to strive for the synthesis of defect-free single crystalline nanoparticles. The particle characteristics have been then primarily varied by their morphological features such as size and shape. In this progress report we have compiled recent findings indicating an alternative approach for improving magnetic particle properties. Inspired by other research fields such a semiconductors and perovskite solar cells, we here attempt to redirect the attention of the magnetic nanoparticle community toward exploiting defect-engineering in iron oxide nanoparticles to enhance and adapt particle magnetic properties for *in-vivo* magnetic hyperthermia. Recent experimental and computational studies emphasize a clear benefit of structural defects and associated magnetic spin disorder in various biomedical applications. Defect-rich iron oxide

nanoparticles appear particularly promising candidates for intracellular magnetic hyperthermia and magnetic-heating-triggered drug delivery, wherein transducing heat based on the Néel magnetic relaxation mechanism is crucial. Sharing similar nanomagnetism principles to magnetic hyperthermia^[157], magnetic particle imaging (MPI), an emerging molecular imaging modality, will largely benefit from defect-engineering in iron oxide nanoparticles. The research on developing iron oxide based tracers for MPI is growing rapidly owing to outstanding features of MPI compared to MRI such as high sensitivity, deep tissue imaging, and capability of live imaging^[158]. It is well known that the MPI imaging technique works based on the Néel relaxation mechanism. Therefore, iron oxide nanoparticles with the characteristics highlighted here for defect-rich iron oxide nanoparticles, that is large magnetic susceptibility and low magnetic anisotropy, are well suited for MPI. This correlation was verified by several studies which conclude that nanoflowers are excellent candidates for MPI^[38,39].

We have here summarized studies on synthesis of defect-rich iron oxide nanoparticles, yet our focus is on those studies in which defects and disorder have been mainly included deliberately. We have highlighted few one-pot synthesis reactions and post synthesis thermal treatments in organic solvents and aqueous media that promote structural defects and compositional discontinuities in iron oxide nanoparticles. Anti-phase boundaries, stacking faults, grain boundaries, and twinning defects have been induced in iron oxide nanoparticles.

Looking into the correlation between structural and magnetic lattice, we have realized that one important aspect that is often overlooked is the different characteristics of spin disorder on nanoscale and atomistic length scales. The magnetic structure of iron oxide nanoparticles is directly determined by their structural features, implying that structural defects lead to disordered magnetic lattice and eventual modification of the magnetic properties. Despite the progress in

atomistic analyses, the precise characterization of spin disorder within the particles remains one of the key challenges in nanomagnetism. However, it is crucial to distinguish between surface-induced nanoscale spin disorder and atomistic, structurally induced intraparticle spin disorder when assessing macroscopic magnetic properties and hence technological performance of magnetic nanoparticles.

Admittedly, the programmed defect inclusion in iron oxide nanoparticles is yet in its infant stage, when compared to other fields such as semiconductor technology. However, the number of research articles on revealing and harnessing positive contribution of defects is rapidly growing. In the following, we add our perspectives and ideas on how to systematically engineer defects into the crystal structure of iron oxide nanoparticles.

One of the potential approaches to synthesize iron oxide nanoparticles with grain boundaries like nanoflowers discussed here, is to use a combination of short and long capping ligands with different binding affinity to iron. A combination of short phosphonate-based and oleic acid ligands in thermal decomposition synthesis could lead to the formation of iron oxide nanoparticles with grain boundaries via competitive ligand binding to different positions on particles. The nature of binding between capping ligands and particles is yet largely unknown and thus more elucidations in this regard will facilitate designing disorder in iron oxide nanoparticles.

We envision a great opportunity in combining crystalline disorder and *in-vivo* clearance of magnetic nanoparticles in developing defect-rich nano-heaters and MPI tracers. We believe a novel synthetic approach could be to fabricate nanoparticle organic frameworks (NOFs), wherein nanoparticles are assembled together with responsive molecules such as peptides and short oligonucleotides. Controlling size and polydispersity of these assemblies, NOFs behave similar to nanoflowers and excel at intracellular magnetic hyperthermia. The unique feature of NOFs, non-

existent in nanoflowers, is the capability of being dissociated to small building blocks that can be easily cleared from the body. NOFs will be particularly promising for magnetic monitoring of drug release, wherein a frequent injection of nanocarriers e.g. once a week and thus a rapid clearance of previously administrated nanocarriers is needed to not interfere with newly coming ones in terms of magnetic signal.

A further strategy is doping-induced-defects by replacing iron with magnetic and nonmagnetic cations such as Cu, Co, Zn, or Gd^[159,160]. Doping in iron oxide nanoparticles has traditionally been mainly used to reduce compensating magnetic couplings and improve magnetization, as in the case of Zn²⁺ in iron oxide nanoparticles. We envision the opportunity of inducing other defects and thus tailoring magnetic anisotropy of nanoparticles by defect-induced distortion of the magnetic lattice. Doping appeared as a powerful tool to improve electrical properties of semiconductors^[6] and modify photonic properties of quantum dots^[161]. Studies on doping-induced-defects in iron oxide nanoparticles seem to lack behind other technological fields, which call for employing a combination of atomistic analyses to unveil defects and their impacts on magnetic properties in near future to come.

To sum up, we advocate our review will stimulate further research and development on novel synthetic routes for defect-engineering as well as selecting appropriate characterization methods depending on the type of defect in magnetic nanoparticles. Eliminating the negative connotation associated with defects and disorder in magnetic nanoparticles, our report will set the scene for embracing the structural and magnetic lattice disorders in magnetic nanoparticles to further advance *in-vivo* biomedical applications.

Acknowledgements

S.D. acknowledges financial support from the German Research Foundation (DFG Grant DI 1788/2-1). A.L. acknowledges the Alexander von Humboldt Foundation for postdoctoral research fellowship. P. B. acknowledges financial support from the National Research Fund of Luxembourg (CORE SANS4NCC grant). All three authors contributed equally to the manuscript.

References

1. Estreicher SK. Defect theory: elusive state-of-the-art. *Mater Today* 2003;6(6):26–35.
2. Márk GI, Vértésy Z, Kertész K, Bálint Z, Biró LP. Order-disorder effects in structure and color relation of photonic-crystal-type nanostructures in butterfly wing scales. *Phys Rev E* 2009;80(5):051903.
3. Vukusic P, Hallam B, Noyes J. Brilliant whiteness in ultrathin beetle scales. *Science* (80-) 2007;315(5810):348.
4. Lurie-Luke E. Product and technology innovation: What can biomimicry inspire? *Biotechnol Adv* 2014;32(8):1494–505.
5. Wiersma DS. Disordered photonics. *Nat Photonics* 2013;7(3):188–96.
6. Queisser HJ, Haller EE. Defects in semiconductors: Some fatal, some vital. *Science* (80-) [Internet] 1998;281(5379):945–50. Available from: <http://science.sciencemag.org/>
7. Yin WJ, Shi T, Yan Y. Unusual defect physics in CH₃NH₃PbI₃ perovskite solar cell absorber. *Appl Phys Lett* 2014;104(6):063903.
8. Li X, Lu K. Playing with defects in metals. *Nat Mater* 2017;16(7):700–1.
9. Rojac T, Bencan A, Drazic G, Sakamoto N, Ursic H, Jancar B, et al. Domain-wall conduction in ferroelectric BiFeO₃ controlled by accumulation of charged defects. *Nat Mater* 2017;16(3):322–7.
10. Shyu TC, Damasceno PF, Dodd PM, Lamoureux A, Xu L, Shlian M, et al. A kirigami approach to engineering elasticity in nanocomposites through patterned defects. *Nat Mater* 2015;14(8):785–9.
11. Krasheninnikov A V., Banhart FJ. Engineering of nanostructured carbon materials with electron. *Nat Mater* 2007;6(10):723–33.
12. Wei Y, Wu J, Yin H, Shi X, Yang R, Dresselhaus M. The nature of strength enhancement and weakening by pentagong-heptagon defects in graphene. *Nat Mater* 2012;11(9):759–63.
13. Cairns AB, Goodwin AL. Structural disorder in molecular framework materials. *Chem Soc Rev* 2013;42(12):4881–93.
14. Keen DA, Goodwin AL. The crystallography of correlated disorder. *Nature* 2015;521(7552):303–9.
15. Overy AR, Cairns AB, Cliffe MJ, Simonov A, Tucker MG, Goodwin AL. Design of crystal-like aperiodic solids with selective disorder-phonon coupling. *Nat Commun* 2016;7.
16. Simonov A, De Baerdemaeker T, Boström HLB, Ríos Gómez ML, Gray HJ, Chernyshov D, et al. Hidden diversity of vacancy networks in Prussian blue analogues. *Nature* 2020;578(7794):256–60.

17. Zhang Y, Stocks GM, Jin K, Lu C, Bei H, Sales BC, et al. Influence of chemical disorder on energy dissipation and defect evolution in concentrated solid solution alloys. *Nat Commun* 2015;6:8736.
18. Mrudul MS, Tancogne-Dejean N, Rubio A, Dixit G. High-harmonic generation from spin-polarised defects in solids. *npj Comput Mater* [Internet] 2020;6(1):10. Available from: <http://www.nature.com/articles/s41524-020-0275-z>
19. Friedberg R, Paul DI. New Theory of Coercive Force of Ferromagnetic Materials. *Phys Rev Lett* 1975;34:1234.
20. Michels A, Mettus D, Titov I, Malyeyev A, Bersweiler M, Bender P, et al. Microstructural-defect-induced Dzyaloshinskii-Moriya interaction. *Phys Rev B* 2019;99(1):014416.
21. Mühlbauer S, Binz B, Jonietz F, Pfleiderer C, Rosch A, Neubauer A, et al. Skyrmion Lattice in a Chiral Magnet. *Science* (80-) [Internet] 2009;323:915–9. Available from: <http://science.sciencemag.org/>
22. Sander D, Valenzuela SO, Makarov D, Marrows CH, Fullerton EE, Fischer P, et al. The 2017 Magnetism Roadmap. *J Phys D Appl Phys* 2017;50(36):363001.
23. Lu A-H, Salabas EL, Schüth F. Magnetic nanoparticles: synthesis, protection, functionalization, and application. *Angew Chem Int Ed Engl* [Internet] 2007 [cited 2014 Apr 28];46(8):1222–44. Available from: <http://www.ncbi.nlm.nih.gov/pubmed/17278160>
24. Pankhurst QA, Connolly J, Jones SK, Dobson J. Applications of magnetic nanoparticles in biomedicine. *J Phys D Appl Phys* 2003;36:167–81.
25. Jordan A, Felix R. Magnetic fluid hyperthermia (MFH): Cancer treatment with AC magnetic field induced excitation of biocompatible superparamagnetic nanoparticles. *J Magn Magn Mater* [Internet] 1999;201:413–9. Available from: <https://www.researchgate.net/publication/320610684>
26. Gleich B, Weizenecker J. Tomographic imaging using the nonlinear response of magnetic particles. *Nature* 2005;435(7046):1214–7.
27. Cunningham CH, Arai T, Yang PC, McConnell M V., Pauly JM, Conolly SM. Positive contrast magnetic resonance imaging of cells labeled with magnetic nanoparticles. *Magn Reson Med* 2005;53(5):999–1005.
28. Muscas G, Yaacoub N, Peddis D. Magnetic Disorder in Nanostructured Materials. In: *Novel Magnetic Nanostructures*. Elsevier; 2018. page 127–63.
29. Oh MH, Cho MG, Chung DY, Park I, Kwon YP, Ophus C, et al. Design and synthesis of multigrain nanocrystals via geometric misfit strain. *Nature* [Internet] 2020;577(7790):359–63. Available from: <http://www.nature.com/articles/s41586-019-1899-3>
30. Massart R. Preparation of Aqueous Magnetic Liquids in Alkaline and Acidic Media. *IEEE Trans Magn* 1981;34(2):142.
31. Baaziz W, Pichon BP, Fleutot S, Liu Y, Lefevre C, Greneche JM, et al. Magnetic iron oxide nanoparticles: Reproducible tuning of the size and nanosized-dependent composition, defects, and spin canting. *J Phys Chem C* 2014;118(7):3795–810.
32. Hugounenq P, Levy M, Alloyeau D, Lartigue L, Dubois E, Cabuil V, et al. Iron oxide monocrystalline nanoflowers for highly efficient magnetic hyperthermia. *J Phys Chem C* 2012;116(29):15702–12.
33. Lartigue L, Hugounenq P, Alloyeau D, Clarke SP, Lévy M, Bacri JC, et al. Cooperative organization in iron oxide multi-core nanoparticles potentiates their efficiency as heating

- mediators and MRI contrast agents. *ACS Nano* 2012;6(12):10935–49.
34. Sakellari D, Brintakis K, Kostopoulou A, Myrovali E, Simeonidis K, Lappas A, et al. Ferrimagnetic nanocrystal assemblies as versatile magnetic particle hyperthermia mediators. *Mater Sci Eng, C* 2016;58:187–93.
 35. Bender P, Fock J, Frandsen C, Hansen MF, Balceris C, Ludwig F, et al. Relating Magnetic Properties and High Hyperthermia Performance of Iron Oxide Nanoflowers. *J Phys Chem C* 2018;122(5):3068–77.
 36. Bender P, Fock J, Hansen MF, Bogart LK, Southern P, Ludwig F, et al. Influence of clustering on the magnetic properties and hyperthermia performance of iron oxide nanoparticles. *Nanotechnology* 2018;29(42):425705.
 37. Lak A, Cassani M, Mai BT, Winkelmann N, Cabrera D, Sadrollahi E, et al. Fe²⁺ Deficiencies, FeO Subdomains, and Structural Defects Favor Magnetic Hyperthermia Performance of Iron Oxide Nanocubes into Intracellular Environment. *Nano Lett* 2018;18(11):6856–66.
 38. Kratz H, Mohtashamdolatshahi A, Eberbeck D, Kosch O, Hauptmann R, Wiekhorst F, et al. Mpi phantom study with a high-performing multicore tracer made by coprecipitation. *Nanomaterials* 2019;9(10):1466.
 39. Wetegrove M, Witte K, Bodnar W, Pfahl DE, Springer A, Schell N, et al. Formation of maghemite nanostructures in polyol: tuning the particle size via the precursor stoichiometry. *CrystEngComm* 2019;21(12):1956–66.
 40. Cazares-Cortes E, Cabana S, Boitard C, Nehlig E, Griffete N, Fresnais J, et al. Recent insights in magnetic hyperthermia: From the “hot-spot” effect for local delivery to combined magneto-photo-thermia using magneto-plasmonic hybrids. *Adv Drug Deliv Rev* 2019;138:233–46.
 41. Périgo EA, Hemery G, Sandre O, Ortega D, Garaio E, Plazaola F, et al. Fundamentals and advances in magnetic hyperthermia. *Appl Phys Rev* 2015;2(4):041302.
 42. Bordet A, Lacroix L-M, Fazzini P-F, Carrey J, Soulantica K, Chaudret B. Magnetically Induced Continuous CO₂ Hydrogenation Using Composite Iron Carbide Nanoparticles of Exceptionally High Heating Power. *Angew Chem* 2016;128(51):16126–30.
 43. Niether C, Faure S, Bordet A, Deseure J, Chatenet M, Carrey J, et al. Improved water electrolysis using magnetic heating of FeC–Ni core–shell nanoparticles. *Nat Energy* [Internet] 2018;3(6):476–83. Available from: <http://www.nature.com/articles/s41560-018-0132-1>
 44. Urraca JL, Cortés-Llanos B, Aroca C, de la Presa P, Pérez L, Moreno-Bondi MC. Magnetic Field-Induced Polymerization of Molecularly Imprinted Polymers. *J Phys Chem C* 2018;122(18):10189–96.
 45. Mahmoudi K, Hadjipanayis CG. The application of magnetic nanoparticles for the treatment of brain tumors. *Front Chem* 2014;2:1–5.
 46. Beola L, Gutiérrez L, Grazú V, Asín L. A Roadmap to the Standardization of In Vivo Magnetic Hyperthermia. In: *Nanomaterials for Magnetic and Optical Hyperthermia Applications*. Elsevier; 2019. page 317–37.
 47. Blanco-Andujar C, Teran FJ, Ortega D. Current Outlook and Perspectives on Nanoparticle-Mediated Magnetic Hyperthermia. In: *Iron Oxide Nanoparticles for Biomedical Applications*. Elsevier; 2018. page 197–245.
 48. Wells J, Kazakova O, Posth O, Steinhoff U, Petronis S, Bogart LK, et al. Standardisation of magnetic nanoparticles in liquid suspension. *J Phys D Appl Phys* 2017;50(38):383003.

49. Di Corato R, Espinosa A, Lartigue L, Tharaud M, Chat S, Pellegrino T, et al. Magnetic hyperthermia efficiency in the cellular environment for different nanoparticle designs. *Biomaterials* 2014;35(24):6400–11.
50. Ota S, Yamada T, Takemura Y. Magnetization reversal and specific loss power of magnetic nanoparticles in cellular environment evaluated by AC hysteresis measurement. *J Nanomater* 2015;2015:836761.
51. Cabrera D, Coene A, Leliaert J, Artés-Ibáñez EJ, Dupré L, Telling ND, et al. Dynamical Magnetic Response of Iron Oxide Nanoparticles Inside Live Cells. *ACS Nano* 2018;12(3):2741–52.
52. Ortega D, Pankhurst QA. Magnetic hyperthermia. 2012. page 60–88.
53. Mahmoudi K, Bouras A, Bozec D, Ivkov R, Hadjipanayis C. Magnetic hyperthermia therapy for the treatment of glioblastoma: a review of the therapy's history, efficacy and application in humans. *Int. J. Hyperth.* 2018;34(8):1316–28.
54. Dennis CL, Ivkov R. Physics of heat generation using magnetic nanoparticles for hyperthermia. *Int J Hyperth* 2013;29(8):715–29.
55. Kallumadil M, Tada M, Nakagawa T, Abe M, Southern P, Pankhurst QA. Suitability of commercial colloids for magnetic hyperthermia. *J Magn Magn Mater* 2009;321(10):1509–13.
56. Wildeboer RR, Southern P, Pankhurst QA. On the reliable measurement of specific absorption rates and intrinsic loss parameters in magnetic hyperthermia materials. *J Phys D Appl Phys* 2014;47(49):495003.
57. Rosensweig RE. Heating magnetic fluid with alternating magnetic field. *J Magn Magn Mater* 2002;252:370–4.
58. Fortin JP, Wilhelm C, Servais J, Ménager C, Bacri JC, Gazeau F. Size-sorted anionic iron oxide nanomagnets as colloidal mediators for magnetic hyperthermia. *J Am Chem Soc* 2007;129(9):2628–35.
59. Andreu I, Urtizberea A, Natividad E. Anisotropic self-assemblies of magnetic nanoparticles: experimental evidence of low-field deviation from the linear response theory and empirical model. *Nanoscale [Internet]* 2020;12(2):572–83. Available from: <http://xlink.rsc.org/?DOI=C9NR05946F>
60. Déjardin JL, Vernay F, Respaud M, Kachkachi H. Effect of dipolar interactions and DC magnetic field on the specific absorption rate of an array of magnetic nanoparticles. *J Appl Phys* 2017;121(20):203903.
61. Simeonidis K, Morales MP, Marciello M, Angelakeris M, De La Presa P, Lazaro-Carrillo A, et al. In-situ particles reorientation during magnetic hyperthermia application: Shape matters twice. *Sci Rep* 2016;6:38382.
62. Shi G, Takeda R, Trisnanto SB, Yamada T, Ota S, Takemura Y. Enhanced specific loss power from Resovist® achieved by aligning magnetic easy axes of nanoparticles for hyperthermia. *J Magn Magn Mater* 2019;473:148–54.
63. Lappas A, Antonaropoulos G, Brintakis K, Vasilakaki M, Trohidou KN, Iannotti V, et al. Vacancy-Driven Noncubic Local Structure and Magnetic Anisotropy Tailoring in Fe₃-δ O₄ Nanocrystals. *Phys Rev X* 2019;9(4):041044.
64. Muela A, Muñoz D, Martín-Rodríguez R, Orue I, Garaio E, Abad Díaz De Cerio A, et al. Optimal Parameters for Hyperthermia Treatment Using Biomineralized Magnetite Nanoparticles: Theoretical and Experimental Approach. *J Phys Chem C* 2016;120(42):24437–48.

65. Herzer G. Grain size dependence of coercivity and permeability in nanocrystalline ferromagnets. *IEEE Trans Magn* 1990;26(5):1397–402.
66. Herzer G. Soft magnetic nanocrystalline materials. *Scr Met Mater* 1995;33:1741–56.
67. Ding J, Li Y, Chen LF, Deng CR, Shi Y, Chow YS, et al. Microstructure and soft magnetic properties of nanocrystalline Fe-Si powders. *J Alloy Compd* [Internet] 2001;314:262–7. Available from: www.elsevier.com/locate/jallcom
68. Zeng Q, Baker I, McCreary V, Yan Z. Soft ferromagnetism in nanostructured mechanical alloying FeCo-based powders. *J Magn Magn Mater* 2007;318(1–2):28–38.
69. Kolen'Ko Y V., Bañobre-López M, Rodríguez-Abreu C, Carbó-Argibay E, Sailsman A, Piñeiro-Redondo Y, et al. Large-scale synthesis of colloidal Fe₃O₄ nanoparticles exhibiting high heating efficiency in magnetic hyperthermia. *J Phys Chem C* 2014;118(16):8691–701.
70. Negi DS, Sharona H, Bhat U, Palchoudhury S, Gupta A, Datta R. Surface spin canting in Fe₃O₄ and CoFe₂O₄ nanoparticles probed by high-resolution electron energy loss spectroscopy. *Phys Rev B* 2017;95(17):174444.
71. Nedelkoski Z, Kepaptsoglou D, Lari L, Wen T, Booth RA, Oberdick SD, et al. Origin of reduced magnetization and domain formation in small magnetite nanoparticles. *Sci Rep* 2017;7:45997.
72. Castellanos-Rubio I, Rodrigo I, Munshi R, Arriortua O, Garitaonandia JS, Martinez-Amesti A, et al. Outstanding heat loss via nano-octahedra above 20 nm in size: From wustite-rich nanoparticles to magnetite single-crystals. *Nanoscale* 2019;11(35):16635–49.
73. Simeonidis K, Martinez-Boubeta C, Serantes D, Ruta S, Chubykalo-Fesenko O, Chantrell R, et al. Controlling Magnetization Reversal and Hyperthermia Efficiency in Core-Shell Iron-Iron Oxide Magnetic Nanoparticles by Tuning the Interphase Coupling. *ACS Appl Nano Mater* 2020;
74. Wetterskog E, Tai CW, Grins J, Bergström L, Salazar-Alvarez G. Anomalous magnetic properties of nanoparticles arising from defect structures: Topotaxial oxidation of Fe_{1-x}O|Fe_{3-δ}O₄ core|shell nanocubes to single-phase particles. *ACS Nano* 2013;7(8):7132–44.
75. Testa-Anta M, Rodríguez-González B, Salgueiriño V. Partial FeO–Fe₃O₄ Phase Transition Along the <111> Direction of the Cubic Crystalline Structure in Iron Oxide Nanocrystals. *Part Part Syst Char* 2019;36(11):1900283.
76. Cabrera D, Lak A, Yoshida T, Materia ME, Ortega D, Ludwig F, et al. Unraveling viscosity effects on the hysteresis losses of magnetic nanocubes. *Nanoscale* [Internet] 2017;9:5094–101. Available from: <http://xlink.rsc.org/?DOI=C7NR00810D>
77. Gavilán H, Kowalski A, Heinke D, Sugunan A, Sommertune J, Varón M, et al. Colloidal Flower-Shaped Iron Oxide Nanoparticles: Synthesis Strategies and Coatings. *Part Part Syst Char* 2017;34(7):1700094.
78. Dutz S. Are magnetic multicore nanoparticles promising candidates for biomedical applications? *IEEE Trans Magn* 2016;52(9):0200103.
79. Michels A, Viswanath RN, Barker JG, Birringer R, Weissmüller J. Range of magnetic correlations in nanocrystalline soft magnets. *Phys Rev Lett* 2003;91(26):267204.
80. Ognjanović M, Radović M, Mirković M, Prijović Ž, Puerto Morales M Del, Čeh M, et al. ^{99m}Tc-, ⁹⁰Y-, and ¹⁷⁷Lu-Labeled Iron Oxide Nanoflowers Designed for Potential Use in Dual Magnetic Hyperthermia/Radionuclide Cancer Therapy and Diagnosis. *ACS Appl Mater Interfaces* 2019;11(44):41109–17.

81. Nishimoto K, Ota S, Shi G, Takeda R, Trisnanto SB, Yamada T, et al. High intrinsic loss power of multicore magnetic nanoparticles with blood-pooling property for hyperthermia. *AIP Adv* [Internet] 2019;9:035347. Available from: <https://doi.org/10.1063/1.5079875@adv.2019.JMI2019.issue-1>
82. Shaw SK, Biswas A, Gangwar A, Maiti P, Prajapat CL, Meena SS, et al. Synthesis of exchange coupled nanoflowers for efficient magnetic hyperthermia. *J Magn Magn Mater* 2019;484:437–44.
83. Bender P, Honecker D, Fernández Barquín L. Supraferromagnetic correlations in clusters of magnetic nanoflowers. *Appl Phys Lett* 2019;115(13):132406.
84. Bender P, Wetterskog E, Honecker D, Fock J, Frandsen C, Moerland C, et al. Dipolar-coupled moment correlations in clusters of magnetic nanoparticles. *Phys Rev B* 2018;98(22):224420.
85. Faure B, Wetterskog E, Gunnarsson K, Josten E, Hermann RP, Brückel T, et al. 2D to 3D crossover of the magnetic properties in ordered arrays of iron oxide nanocrystals. *Nanoscale* 2013;5:953–60.
86. Serantes D, Baldomir D, Martinez-Boubeta C, Simeonidis K, Angelakeris M, Natividad E, et al. Influence of dipolar interactions on hyperthermia properties of ferromagnetic particles. *J Appl Phys* 2010;108(7):073918.
87. Fernández-Pacheco A, Streubel R, Fruchart O, Hertel R, Fischer P, Cowburn RP. Three-dimensional nanomagnetism. *Nat. Commun.* 2017;8(1).
88. Daffé N, Choueikani F, Neveu S, Arrio MA, Juhin A, Ohresser P, et al. Magnetic anisotropies and cationic distribution in CoFe₂O₄ nanoparticles prepared by coprecipitation route: Influence of particle size and stoichiometry. *J Magn Magn Mater* 2018;460:243–52.
89. Dutta P, Pal S, Seehra MS, Shah N, Huffman GP. Size dependence of magnetic parameters and surface disorder in magnetite nanoparticles. *J Appl Phys* 2009;105(7):2007–10.
90. Fock J, Bogart LK, González-Alonso D, Espeso JI, Hansen MF, Varón M, et al. On the “centre of gravity” method for measuring the composition of magnetite/maghemite mixtures, or the stoichiometry of magnetite-maghemite solid solutions, via ⁵⁷Fe Mössbauer spectroscopy. *J Phys D Appl Phys* 2017;50(26).
91. Testa-Anta M, Ramos-Docampo MA, Comesaña-Hermo M, Rivas-Murias B, Salgueiriño V. Raman spectroscopy to unravel the magnetic properties of iron oxide nanocrystals for bio-related applications. *Nanoscale Adv* 2019;1(6):2086–103.
92. Daou TJ, Greneche J-M, Lee S-J, Lee S, Lefevre C, Bégin-Colin S, et al. Spin Canting of Maghemite Studied by NMR and In-Field Mössbauer Spectrometry. *J Phys Chem C* [Internet] 2010 [cited 2020 Feb 15];114(19):8794–9. Available from: <https://pubs.acs.org/doi/10.1021/jp100726c>
93. Phatak C, Petford-Long AK, De Graef M. Recent advances in Lorentz microscopy. *Curr Opin Solid State Mater Sci* 2016;20(2):107–14.
94. Golosovsky I V., Tovar M, Hoffman U, Mirebeau I, Fauth F, Kurdyukov DA, et al. Diffraction studies of the crystalline and magnetic structures of γ -Fe₂O₃ iron oxide nanostructured in porous glass. *JETP Lett* 2006;83(7):298–301.
95. Mühlbauer S, Honecker D, Périgo ÉA, Bergner F, Disch S, Heinemann A, et al. Magnetic small-angle neutron scattering. *Rev Mod Phys* [Internet] 2019 [cited 2019 Sep 19];91(1):015004. Available from:

- <https://link.aps.org/doi/10.1103/RevModPhys.91.015004>
96. Kovács A, Sato K, Lazarov VK, Galindo PL, Konno TJ, Hirotsu Y. Direct observation of a surface induced disordering process in magnetic nanoparticles. *Phys Rev Lett* 2009;103(11):1–4.
 97. Curiale J, Granada M, Troiani HE, Sánchez RD, Leyva AG, Levy P, et al. Magnetic dead layer in ferromagnetic manganite nanoparticles. *Appl Phys Lett* [Internet] 2009 [cited 2019 Sep 30];95(4):043106. Available from: <http://aip.scitation.org/doi/10.1063/1.3187538>
 98. Shendruk TN, Desautels RD, Southern BW, Van Lierop J. The effect of surface spin disorder on the magnetism of γ -Fe₂O₃ nanoparticle dispersions. *Nanotechnology* 2007;18(45).
 99. Greneche JM. Structural and Magnetic Properties of Nanostructured Oxides Investigated by ⁵⁷Fe Mössbauer Spectrometry. *Hyperfine Interact* 2003;148–149(1–4):79–89.
 100. Coey JMD. Noncollinear spin arrangement in ultrafine ferrimagnetic crystallites. *Phys Rev Lett* 1971;27(17):1140–2.
 101. Kodama RH, Berkowitz AE, McNiff EJ, Foner S. Surface Spin Disorder in NiFe₂O₄ Nanoparticles. *Phys Rev Lett* 1996;77(2):394–7.
 102. Kodama RH, Berkowitz AE. Atomic-scale magnetic modeling of oxide nanoparticles. *Phys Rev B* 1999;59(9):6321–36.
 103. Tronc E, Prené P, Jolivet JP, Dormann JL, Grenèche JM. Spin Canting in γ -Fe₂O₃ Nanoparticles. *Hyperfine Interact* 1998;112(1–4):97–100.
 104. Varón M, Beleggia M, Kasama T, Harrison RJ, Dunin-Borkowski RE, Puentes VF, et al. Dipolar Magnetism in Ordered and Disordered Low-Dimensional Nanoparticle Assemblies. *Sci Rep* 2013;3:1234.
 105. Gatel C, Bonilla FJ, Meffre A, Snoeck E, Warot-Fonrose B, Chaudret B, et al. Size-Specific Spin Configurations in Single Iron Nanomagnet: From Flower to Exotic Vortices. *Nano Lett* 2015;15(10):6952–7.
 106. Disch S, Wetterskog E, Hermann RP, Wiedenmann A, Vainio U, Salazar-Alvarez G, et al. Quantitative spatial magnetization distribution in iron oxide nanocubes and nanospheres by polarized small-angle neutron scattering. *New J Phys* 2012;14:013025.
 107. Krycka KL, Booth RA, Hogg CR, Ijiri Y, Borchers JA, Chen WC, et al. Core-shell magnetic morphology of structurally uniform magnetite nanoparticles. *Phys Rev Lett* 2010;104(20):2–5.
 108. Krycka KL, Borchers JA, Booth RA, Ijiri Y, Hasz K, Rhyne JJ, et al. Origin of Surface Canting within Fe₃O₄ Nanoparticles. *Phys Rev Lett* [Internet] 2014;113(14):147203. Available from: <https://link.aps.org/doi/10.1103/PhysRevLett.113.147203>
 109. Krycka KL, Borchers JA, Booth RA, Hogg CR, Ijiri Y, Chen WC, et al. Internal magnetic structure of magnetite nanoparticles at low temperature. *J Appl Phys* [Internet] 2010 [cited 2020 Feb 15];107(9):09B525. Available from: <http://aip.scitation.org/doi/10.1063/1.3358049>
 110. Zakutna D, Niznansky D, Barnsley L, Feoktystov A, Honecker D, Disch S. Field-Dependence of Magnetic Disorder in Nanoparticles. *Phys Rev X* 2020;
 111. Sayed F, Yaacoub N, Labaye Y, Hassan RS, Singh G, Kumar PA, et al. Surface Effects in Ultrathin Iron Oxide Hollow Nanoparticles: Exploring Magnetic Disorder at the Nanoscale. *J Phys Chem C* [Internet] 2018 [cited 2020 Feb 11];122(13):7516–24. Available from: <https://pubs.acs.org/doi/10.1021/acs.jpcc.8b00300>

112. Labaye Y, Crisan O, Berger L, Greneche JM, Coey JMD. Surface anisotropy in ferromagnetic nanoparticles. *J Appl Phys* [Internet] 2002 [cited 2019 Oct 1];91(10):8715. Available from: <http://scitation.aip.org/content/aip/journal/jap/91/10/10.1063/1.1456419>
113. Bersweiler M, Bender P, Vivas LG, Albino M, Petrecca M, Mühlbauer S, et al. Size-dependent spatial magnetization profile of manganese-zinc ferrite $Mn_{0.2}Zn_{0.2}Fe_{2.6}O_4$ nanoparticles. *Phys Rev B* 2019;100(14):0–10.
114. Oberdick SD, Abdelgawad A, Moya C, Mesbahi-Vasey S, Kepaptsoglou D, Lazarov VK, et al. Spin canting across core/shell $Fe_3O_4/MnxFe_{3-x}O_4$ nanoparticles. *Sci Rep* 2018;8(1).
115. Herlitschke M, Disch S, Sergueev I, Schlage K, Wetterskog E, Bergström L, et al. Spin disorder in maghemite nanoparticles investigated using polarized neutrons and nuclear resonant scattering. *J Phys Conf Ser* [Internet] 2016;711:012002. Available from: <http://stacks.iop.org/1742-6596/711/i=1/a=012002?key=crossref.b6d67217cd4ae60661be98085afa4b70>
116. Pacakova B, Kubickova S, Salas G, Mantlikova AR, Marciello M, Morales MP, et al. The internal structure of magnetic nanoparticles determines the magnetic response. *Nanoscale* 2017;9(16):5129–40.
117. Carta D, Casula MF, Falqui A, Loche D, Mountjoy G, Sangregorio C, et al. A Structural and Magnetic Investigation of the Inversion Degree in Ferrite Nanocrystals MFe_2O_4 ($M = Mn, Co, Ni$). *J Phys Chem C* [Internet] 2009 [cited 2019 Sep 23];113(20):8606–15. Available from: <https://pubs.acs.org/doi/10.1021/jp901077c>
118. Carta D, Casula MF, Floris P, Falqui A, Mountjoy G, Boni A, et al. Synthesis and microstructure of manganese ferrite colloidal nanocrystals. *Phys Chem Chem Phys* [Internet] 2010 [cited 2019 Sep 22];12(19):5074. Available from: <http://xlink.rsc.org/?DOI=b922646j>
119. Yang A, Chinnasamy CN, Greneche JM, Chen Y, Yoon SD, Chen Z, et al. Enhanced Néel temperature in Mn ferrite nanoparticles linked to growth-rate-induced cation inversion. *Nanotechnology* [Internet] 2009 [cited 2019 Sep 23];20(18):185704. Available from: <http://stacks.iop.org/0957-4484/20/i=18/a=185704?key=crossref.9dc7f07a35354761a5af15eec186a562>
120. Andersen HL, Saura-Múzquiz M, Granados-Miralles C, Canévet E, Lock N, Christensen M. Crystalline and magnetic structure-property relationship in spinel ferrite nanoparticles. *Nanoscale* 2018;10(31):14902–14.
121. Andersen HL, Granados-Miralles C, Saura-Múzquiz M, Stingaciu M, Larsen J, Søndergaard-Pedersen F, et al. Enhanced intrinsic saturation magnetization of $Zn_xCo_{1-x}Fe_2O_4$ nanocrystallites with metastable spinel inversion. *Mater Chem Front* 2019;3(4):668–79.
122. Fontaiña-Troitiño N, Ramos-Docampo MA, Testa-Anta M, Rodríguez-González B, Bañobre-López M, Bocher L, et al. Antiphase boundaries in truncated octahedron-shaped Zn-doped magnetite nanocrystals. *J Mater Chem C* 2018;6(47):12800–7.
123. Rockenberger J, Scher EC, Alivisatos AP. A new nonhydrolytic single-precursor approach to surfactant-capped nanocrystals of transition metal oxides [15]. *J Am Chem Soc* 1999;121(49):11595–6.
124. Hyeon T, Lee SS, Park J, Chung Y, Na H Bin. Synthesis of Highly Crystalline and Monodisperse Maghemite Nanocrystallites without a Size-Selection Process. *J Am Chem Soc* 2001;123(8):12798–801.

125. Guardia P, Pérez-Juste J, Labarta A, Batlle X, Liz-Marzán LM. Heating rate influence on the synthesis of iron oxide nanoparticles: The case of decanoic acid. *Chem Commun* 2010;46(33):6108–10.
126. Yu WW, Falkner JC, Yavuz CT, Colvin VL. Synthesis of monodisperse iron oxide nanocrystals by thermal decomposition of iron carboxylate salts { . *Chem Commun* 2004;2306–7.
127. Redl FX, Black CT, Papaefthymiou GC, Sandstrom RL, Yin M, Zeng H, et al. Magnetic, electronic, and structural characterization of nonstoichiometric iron oxides at the nanoscale. *J Am Chem Soc* [Internet] 2004;126(44):14583–99. Available from: <http://www.ncbi.nlm.nih.gov/pubmed/15521779>
128. Park J, An K, Hwang Y, Park J-G, Noh H-J, Kim J-Y, et al. Ultra-large-scale syntheses of monodisperse nanocrystals. *Nat Mater* [Internet] 2004;3(12):891–5. Available from: <http://www.nature.com/nmat/journal/v3/n12/full/nmat1251.html%5Cnhttp://www.nature.com/nmat/journal/v3/n12/pdf/nmat1251.pdf>
129. Wang Y, He J, Liu C, Chong WH, Chen H. Thermodynamics versus kinetics in Nanosynthesis. *Angew Chemie - Int Ed* 2015;54(7):2022–51.
130. Roca AG, Gutiérrez L, Gavilán H, Fortes Brollo ME, Veintemillas-Verdaguer S, Morales M del P. Design strategies for shape-controlled magnetic iron oxide nanoparticles. *Adv Drug Deliv Rev* 2019;138:68–104.
131. Shavel A, Rodríguez-González B, Spasova M, Farle M, Liz-Marzán LM. Synthesis and characterization of iron/iron oxide core/shell nanocubes. *Adv Funct Mater* 2007;17(18):3870–6.
132. Lak A, Kraken M, Ludwig F, Kornowski A, Eberbeck D, Sievers S, et al. Size dependent structural and magnetic properties of FeO-Fe₃O₄ nanoparticles. *Nanoscale* 2013;5(24):12286–95.
133. Levy M, Quarta A, Espinosa A, Figuerola A, Wilhelm C, García-Hernández M, et al. Correlating magneto-structural properties to hyperthermia performance of highly monodisperse iron oxide nanoparticles prepared by a seeded-growth route. *Chem Mater* 2011;23:4170–80.
134. Walter A, Billotey C, Garofalo A, Ulhaq-Bouillet C, Lefèvre C, Taleb J, et al. Mastering the shape and composition of dendronized iron oxide nanoparticles to tailor magnetic resonance imaging and hyperthermia. *Chem Mater* 2014;26(18):5252–64.
135. Torruella P, Arenal R, De La Peña F, Saggi Z, Yedra L, Eljarrat A, et al. 3D Visualization of the Iron Oxidation State in FeO/Fe₃O₄ Core-Shell Nanocubes from Electron Energy Loss Tomography. *Nano Lett* 2016;16(8):5068–73.
136. Chen R, Christiansen MG, Sourakov A, Mohr A, Matsumoto Y, Okada S, et al. High-performance ferrite nanoparticles through nonaqueous redox phase tuning. *Nano Lett* 2016;16:1345–51.
137. Kemp SJ, Ferguson RM, Khandhar AP, Krishnan KM. Monodisperse magnetite nanoparticles with nearly ideal saturation magnetization. *RSC Adv* [Internet] 2016;6(81):77452–64. Available from: <http://xlink.rsc.org/?DOI=C6RA12072E>
138. Unni M, Uhl AM, Savliwala S, Savitzky BH, Dhavalikar R, Garraud N, et al. Thermal Decomposition Synthesis of Iron Oxide Nanoparticles with Diminished Magnetic Dead Layer by Controlled Addition of Oxygen. *ACS Nano* 2017;11:2284–303.
139. Pereira C, Pereira AM, Fernandes C, Rocha M, Mendes R, Fernández-García MP, et al. Superparamagnetic MFe₂O₄ (M = Fe, Co, Mn) nanoparticles: Tuning the particle size and

- magnetic properties through a novel one-step coprecipitation route. *Chem Mater* 2012;24(8):1496–504.
140. Kim D, Lee N, Park M, Kim BH, An K, Hyeon T. Synthesis of Uniform Ferrimagnetic Magnetite Nanocubes. *J Am Chem Soc* 2009;131:454–5.
 141. Kovalenko M V., Bodnarchuk MI, Lechner RT, Hesser G, Schäfler F, Heiss W. Fatty acid salts as stabilizers in size- and shape-controlled nanocrystal synthesis: The case of inverse spinel iron oxide. *J Am Chem Soc* 2007;129:6352–3.
 142. Gavilán H, Sánchez EH, Brollo MEF, Asín L, Moerner KK, Frandsen C, et al. Formation Mechanism of Maghemite Nanoflowers Synthesized by a Polyol-Mediated Process. *ACS Omega* 2017;2(10):7172–84.
 143. Lak A, Kahmann T, Schaper SJ, Obel J, Ludwig F, Müller-Buschbaum P, et al. The Dissociation Rate of Acetylacetonate Ligands Governs the Size of Ferrimagnetic Zinc Ferrite Nanocubes. *ACS Appl Mater Interfaces* 2020;12:217–26.
 144. Sun X, Huls NF, Sigdel A, Sun S. Tuning exchange bias in core/shell FeO/Fe₃O₄ nanoparticles. *Nano Lett* [Internet] 2012;12:246–51. Available from: <http://www.ncbi.nlm.nih.gov/pubmed/22713516>
 145. Lak A, Niculaes D, Anyfantis GC, Bertoni G, Barthel MJ, Marras S, et al. Facile transformation of FeO/Fe₃O₄ core-shell nanocubes to Fe₃O₄ via magnetic stimulation. *Sci Rep* [Internet] 2016;6:1–12. Available from: <http://dx.doi.org/10.1038/srep33295>
 146. Lee J-H, Jang J-T, Choi J-S, Moon SH, Noh S-H, Kim J-W, et al. Exchange-coupled magnetic nanoparticles for efficient heat induction. *Nat Nanotechnol* [Internet] 2011 [cited 2015 Jul 10];6(7):418–22. Available from: <http://www.ncbi.nlm.nih.gov/pubmed/21706024>
 147. Lavorato GC, Das R, Xing Y, Robles J, Litterst FJ, Baggio-Saitovitch E, et al. Origin and Shell-Driven Optimization of the Heating Power in Core/Shell Bimagnetic Nanoparticles. *ACS Appl Nano Mater* 2020;3(2):1755–65.
 148. Sartori K, Choueikani F, Gloter A, Begin-Colin S, Taverna D, Pichon BP. Room Temperature Blocked Magnetic Nanoparticles Based on Ferrite Promoted by a Three-Step Thermal Decomposition Process. *J Am Chem Soc* 2019;141(25):9783–7.
 149. Moon SH, Noh SH, Lee JH, Shin TH, Lim Y, Cheon J. Ultrathin Interface Regime of Core-Shell Magnetic Nanoparticles for Effective Magnetism Tailoring. *Nano Lett* 2017;17(2):800–4.
 150. Lee K, Lee S, Ahn B. Understanding High Anisotropic Magnetism by Ultrathin Shell Layer Formation for Magnetically Hard-Soft Core-Shell Nanostructures. *Chem Mater* 2019;31(3):728–36.
 151. Sytnyk M, Kirchschrager R, Bodnarchuk MI, Primetzhofer D, Kriegner D, Ennsner H, et al. Tuning the magnetic properties of metal-oxide nanocrystal heterostructures by cation exchange. *Nano Lett* [Internet] 2013;13:586–93. Available from: <http://www.ncbi.nlm.nih.gov/pubmed/23362940>
 152. Roca AG, Niznansky D, Poltiero-Vejpravova J, Bittova B, González-Fernández MA, Serna CJ, et al. Magnetite nanoparticles with no surface spin canting. *J Appl Phys* 2009;105(11):114309.
 153. Mamei V, Musinu A, Ardu A, Ennas G, Peddis D, Niznansky D, et al. Studying the effect of Zn-substitution on the magnetic and hyperthermic properties of cobalt ferrite nanoparticles. *Nanoscale* 2016;8(19):10124–37.
 154. Jang J, Nah H, Lee J-H, Moon SH, Kim MG, Cheon J. Critical Enhancements of MRI

- Contrast and Hyperthermic Effects by Dopant-Controlled Magnetic Nanoparticles. *Angew Chemie* 2009;121(7):1260–4.
155. Kumar L, Kumar P, Kuncser V, Greculeasa S, Sahoo B, Kar M. Strain induced magnetism and superexchange interaction in Cr substituted nanocrystalline cobalt ferrite. *Mater Chem Phys* [Internet] 2018 [cited 2019 Sep 2];211:54–64. Available from: <https://www.sciencedirect.com/science/article/pii/S0254058418301032?via%3Dihub>
 156. Kumar R, Kar M. Correlation between lattice strain and magnetic behavior in non-magnetic Ca substituted nano-crystalline cobalt ferrite. *Ceram Int* [Internet] 2016 [cited 2019 Sep 2];42(6):6640–7. Available from: <https://www.sciencedirect.com/science/article/pii/S0272884216000353?via%3Dihub>
 157. Hufschmid R, Arami H, Ferguson RM, Gonzales M, Teeman E, Brush LN, et al. Synthesis of phase-pure and monodisperse iron oxide nanoparticles by thermal decomposition. *Nanoscale* [Internet] 2015 [cited 2015 Jun 15];7:11142–54. Available from: <http://www.ncbi.nlm.nih.gov/pubmed/26059262>
 158. Yu EY, Bishop M, Zheng B, Ferguson RM, Khandhar AP, Kemp SJ, et al. Magnetic Particle Imaging: A Novel in Vivo Imaging Platform for Cancer Detection. *Nano Lett* 2017;17:1648–54.
 159. Fernández-Barahona I, Gutiérrez L, Veintemillas-Verdaguer S, Pellico J, Morales MDP, Catala M, et al. Cu-Doped Extremely Small Iron Oxide Nanoparticles with Large Longitudinal Relaxivity: One-Pot Synthesis and in Vivo Targeted Molecular Imaging. *ACS Omega* 2019;4(2):2719–27.
 160. Luengo Y, Roldan MA, Varela M, Herranz F, Morales MP, Veintemillas-Verdaguer S. Doped-Iron Oxide Nanocrystals Synthesized by One-Step Aqueous Route for Multi-Imaging Purposes. *J Phys Chem C* 2019;123(12):7356–65.
 161. Kim D, Shin K, Kwon SG, Hyeon T. Synthesis and Biomedical Applications of Multifunctional Nanoparticles. *Adv. Mater.* 2018;30(49).